ONE-PART ECO-CELLULAR CONCRETE FOR THE PRECAST INDUSTRY: FUNCTIONAL FEATURES AND LIFE CYCLE ASSESSMENT

Alba Font [1], Lourdes Soriano [1], Mauro M. Tashima [2], José Monzó [1], María Victoria Borrachero [1], Jordi Payá [1].

[1] ICITECH – GIQUIMA Group – Grupo de Investigación en Química de los Materiales de Construcción, Instituto de Ciencia y Tecnología del Hormigón, Universitat Politècnica de Valencia, Valencia, Spain.

[2] Universidade Estadual Paulista (UNESP), Faculdade de Engenharia de Ilha Solteira. MAC – Grupo de Pesquisa em Materiais Alternativos de Construção, Ilha Solteira-SP, Brazil.

Abstract

This paper focuses on investigating greener alternatives of cellular concrete technology to fulfil current searches for a shift to circular economy. A novel one-part eco-cellular concrete (ECC-OP) was developed and studied. The one-part alkali activated materials (AAM-OP) and new alkali-activated cellular concrete (AACC) technologies were combined to develop greener alternative of cellular concrete production. The progressive steps from traditional cellular concrete (TCC) based on ordinary Portland cement (OPC) and commercial aluminium powder (A) to a 100% waste-based cellular concrete are presented. Blast furnace slag (BFS) was the precursor, RHA was employed as the silica source, olive stone biomass ash (OBA) was the alkali source and recycled aluminium foil (A_R) was employed as an aerating agent. The functional features of the materials were studied and compared to those established by the European standard and the American Concrete Institute (ACI) Committee 523 guides. The new ECC-OP with a bulk density, compressive strength and thermal conductivity that respectively equal 660 kg/m^3, 6.3 MPa and 0.20 W/mK was obtained. Finally, a cradle-to-gate life cycle assessment (LCA) was made, where the industrial process of a masonry unit manufacture was raised by using each studied material. A 96% reduction in the kgCO_2eq per m^3 of material was reached with the new proposed ECC-OP compared to TCC manufacturing.

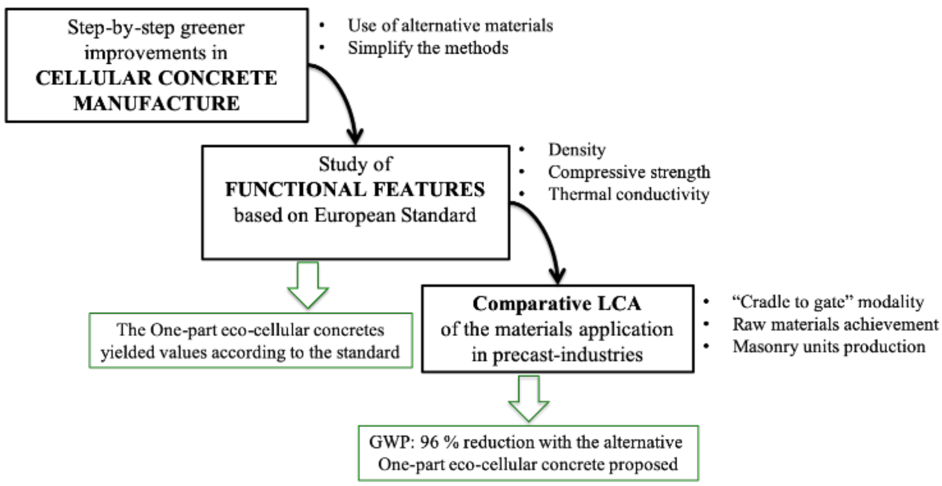

Graphical abstract

Keywords: One-part alkali-activated material, cellular concrete, life cycle assessment, CO_2 emissions, blast furnace slag, biomass ash.

Abbreviations:

TCC: Traditional cellular concrete

AACC: Alkali-activated cellular concrete

ECC: Eco-cellular concrete

ECC-OP: One-part eco-cellular concrete

OPC: Ordinary Portland Cement

BFS: Blast furnace slag

OBA: Olive stone biomass ash

RHA: Rice husk ash

A: Commercial aluminium powder

A_R: Recycled aluminium foil

LCA: Life cycle assessment

GWP: Global Warming Potential relative to CO_2

100-GWP: 100-year GWP time horizon

1. Introduction

Today the concrete industry needs a greener and economic evolution in both raw materials and the manufacturing method. Concrete is the most employed construction material in the world (Colangelo et al., 2018; Van Den Heede and De Belie, 2012). In the European Union (EU), buildings have a strong socio-economic impact by having 40% energy demands, 36% CO_2 emissions, 50% non-renewable raw materials and 35% waste (Novais et al., 2019; Zabalza Bribián et al., 2011). Consequently, the search for a circular economy system is growing for its industrial application (Funfación Conama - Grupo de trabajo GT-6, 2018; Hogeling and Derjanecz, 2018; Schroeder et al., 2018). In recent years, global institutions have opted for the precast construction concept and the responsible use of waste, materials, soil, water, air and power sources (Dahmen et al., 2018).

Traditional cellular concretes (TCC) are low-density insulating materials whose importance is increasing by reducing the volume of material requirements and their suitability in precast industry applications (Chica and Alzate, 2019; Hajimohammadi et al., 2017; Mak et al., 2008; Pytlik and Saxena, 1992). The typical relationship among the natural density (wet weight/volume), compressive strength and thermal conductivity of autoclaved cellular concretes to their application in pre-cast construction elements (in structural and non-structural elements) is shown in Table 1.

Table 1. Relationship between the physical characteristics of the cellular concretes commonly described by authors. Adapted from Dolton and Hannah (Dolton and Hannah, 2006).

Density (kg/m^3)	Compressive strength (MPa)	Thermal conductivity (W/mK)
600	1.98	0.097
550	1.51	0.092
500	1.14	0.086
450	0.84	0.080
400	0.71	0.075

Precast cellular concrete is presented as an interest alternative to develop a greener construction activity. Notwithstanding, environmental issues are commonly linked with TCC components and their manufacture process: i) the main component is ordinary Portland cement (OPC), which is well-known for its major environmental impacts (considerable use of energy and non-renewable raw materials, and around 8% of the world's anthropogenic CO_2 emissions) (Luukkonen et al., 2018a); ii) commercial aluminium powder (A) was the most employed aerating agent, and its production process involves serious environmental issues (Alba Font et al., 2017); iii) the curing treatment of TCC is currently carried out in autoclaves under high temperature and pressure conditions. Thus, strong enviro-economic impacts are associated (Esmaily and Nuranian, 2012; Keawpapasson et al., 2014).

Greener alternatives have been studied in recent years by applying alkali-activated material (AAM) (high-calcium hydraulic precursors) and geopolymer (low-calcium aluminosilicate precursors) technologies in alternative cellular concrete manufacturing, commonly known as the new alkali-activated cellular concretes (AACC) (Hajimohammadi et al., 2017; He et al., 2019; Yang et al., 2014) and geopolymer cellular concretes (GCC), respectively (Bai and Colombo, 2018; Alba Font et al., 2017; Hassan et al., 2018; Novais et al., 2016; Xuan et al., 2019). These systems are characterised by being prepared to avoid autoclave treatment: cellular systems with low density and appropriate compressive strength may be achieved under soft curing conditions. Blast furnace slag (BFS) was employed as a precursor in AACC and A was used as an aerating agent (Esmaily and Nuranian, 2012). The synthesised AACC were cured at 70ºC, 78ºC and 87ºC to achieve density and compressive strength of 953 kg/m^3 and 3.7 MPa after 28 days, respectively. Font et al. developed GCCs based on fluid catalytic cracking catalyst residue (FCC), which was aerated with recycled aluminium foil (Alba Font et al., 2017). The new GCC specimens yielded 600-700 kg/m^3, 2.5-3.5 MPa and 0.581 W/mK after 7 curing days at room temperature.

The most recent research into low CO_2 materials (AAM and geopolymers) has focused on searching for 100% waste-based materials by replacing the required commercial chemical reagents: high alkali hydroxides (NaOH or KOH) and sodium or potassium silicate sources (Choo et al., 2016; de Moraes Pinheiro et al., 2018; Peys et al., 2016). In cellular concrete technology, this concern has been recently introduced. Kamseu et al. manufactured AACC aerated with A by employing rice husk ash or volcanic ash (RHA or VPA) combined with metakaolin activated with a highly concentrated NaOH (8 M) solution (Kamseu et al., 2015). Samples were cured at room temperature for 7 days, and yielded a total porosity exceeding 50%. RHA was also employed (as a silica source) combined with KOH in the alkali-activating reagent preparation for FA-based cellular concretes (Ziegler et al., 2016). The designed samples were aerated by adding A within the 0.05-0.3% range and were cured for 24 h at 50ºC before being stored at room temperature until 60 days. GCCs, aerated with 0.2% of A, had an apparent porosity within the 54–63% range and compressive strength within the 2–2.5 MPa range. The use of RHA as a silica source in preparing the alkali-activating reagent in the FCC-based GCCs and BFS-based AACCs systems was firstly introduced by Font et al. (Font et al., 2018). These authors compared TCCs to the GCCs and AACCs activated with: NaOH/sodium silicate aqueous solution; ii) NaOH/RHA aqueous suspension (for this option, the resulting cellular concrete was called new eco-cellular concretes, ECC). In the new ECC systems, the employed aerating agent was recycled aluminium foil, added before the milling treatment of the precursors. The resulting new ECC specimens had ranges of 782–611 kg/m^3 for density, 3.2–4.6 MPa for compressive strength and 0.113/0.224 W/mK for thermal conductivity after 28 curing days at room temperature, which allowed the reduction of 74-78% of CO_2 emissions *versus* TCC when FCC or BFS was used as a precursor. Stoleriu et al. presented materials based on BFS partially replaced with waste glass powder activated by an NaOH solution, where high porosity was induced by thermal treatment at 900–1,000ºC for 30-60 minutes (Stoleriu et al., 2019).

Olive stone biomass ash (OBA) has been quite recently introduced as a KOH replacement for BFS activation (de Moraes Pinheiro et al., 2018; A. Font et al., 2017). A 100% waste-based material based on new ternary BFS/OBA/RHA systems has been developed with good properties and a high environmental improvement potential (Font et al., 2020). There are not found previous investigations where the alternative alkaline source was introduced to the cellular concrete development.

For pre-cast applications in the concrete industry, the development of one-part AAM has been potentially studied to avoid technical disadvantages while preparing the alkali activator solution (difficulties because large amounts are handled given its corrosiveness and viscosity) (Luukkonen et al., 2018b; Ma et al., 2019; Sturm et al., 2016). These one-part materials consist in a unique solid phase formed by a precursor and alkali source mix, which only needs water as the liquid phase, and is similar to using OPC. Recently, Luukkonen et al. published a review about this initiative to search for close-to-the-market projects of alternative low-carbon materials (Luukkonen et al., 2018a). To the best of our knowledge, there are no published research works that combine the innovations of one-part concretes and ECC technologies.

The aim of the present research was the development of a new cellular concrete based on 100 % waste-materials in which manufacture procedure lead the nearly-zero energy consumption: the new one-part eco-cellular concretes (ECC-OP). These innovative materials are studied to be applied to precast industries as masonry units. Five different typologies of cellular concretes were designed and studied for which step-by-step greener improvements were introduced from TCC to the one-part 100% waste-based eco-cellular concrete production. A study about the functional features of the materials obtained in each step was carried out and compared with the values set by the European standard and by the American Concrete Institute (ACI) Committee 523 guides (AENOR, 2016a; Babbitt et al., 2014). The application of the compared cellular concretes as a masonry unit was assessed and a comparative cradle-to-gate modality life cycle assessment (LCA) was carried out, where the contribution of the new one-part ECC to circular economy was evaluated.

2. Experimental procedure

In this research, the step-by-step development of one-part eco-cellular concrete (ECC) is presented. In Fig. 1, the outline of the followed procedure is shown and the used samples/acronyms are explained.

In this diagram (Fig.1), the compared samples are boxed and the directional black arrow indicates the steps of the introduced improvements. For each step, negative factors (red arrows) and positive factors (green arrows) are indicated: these factors were considered taking into account the harmful/beneficial effects on the preparation of the compared cellular concretes. For example, comparing CA and BA cellular concretes (first step), the red arrow related to "autoclave" means that this harmful factor was eliminated and, in contrast, the green arrow related to "room temperature" means a positive factor in the preparation of the new concrete; the red arrow related to "NaOH/WG" mean that the use of these chemical reagents in the dosage for the new proposed BA cellular concrete corresponds to a harmful contribution.

The direction of the arrows shows if the factor was introduced or removed in the following alternative cellular concrete.

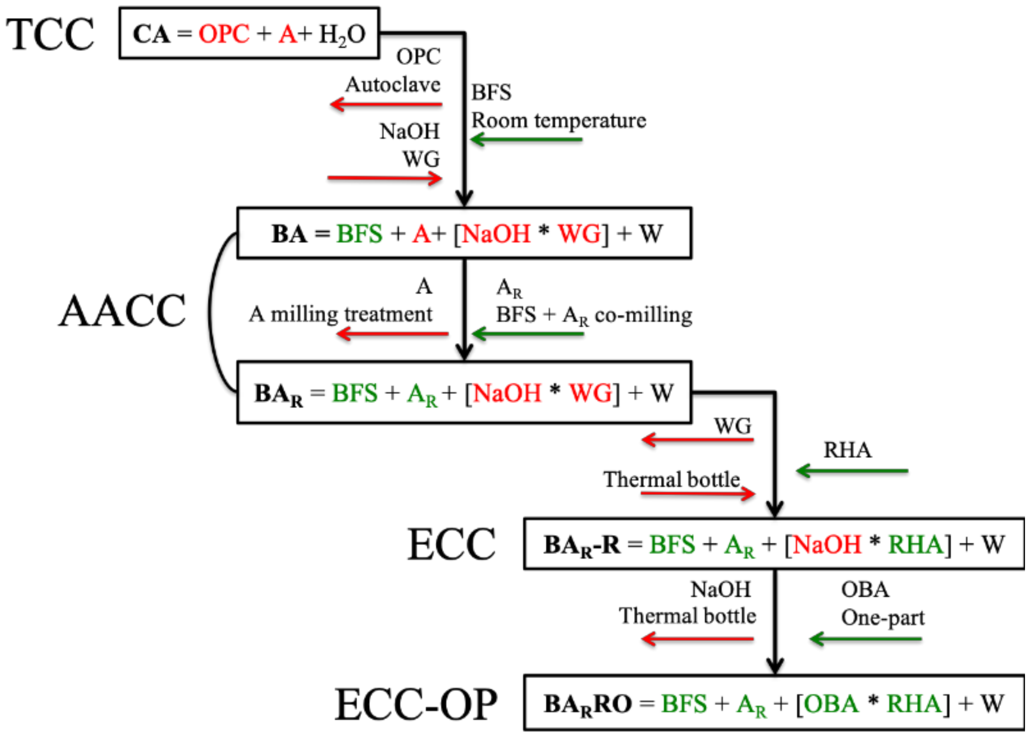

Fig. 1. Outline of the step-by-step improvement introduced into cellular concrete (The negative factors are plotted as red arrows and the positive ones as green arrows).

List of acronyms:

CA: Traditional cellular concrete (TCC) based on ordinary Portland cement (OPC) and water (W), aerated with commercial aluminium powder (A)

BA: Alkali-activated cellular concrete (AACC) based on blast furnace slag (BFS) activated with a sodium hydroxide/sodium silicate (NaOH/WG) solution, aerated with commercial aluminium powder (A)

BA_R: Alkali-activated cellular concrete (AACC) based on blast furnace slag (BFS) activated with a sodium hydroxide/sodium silicate (NaOH/WG) solution, aerated with recycled aluminium foil (A_R)

BA_R-R: Eco-cellular concrete (ECC) based on blast furnace slag (BFS) activated with a sodium hydroxide/rice husk ash (NaOH/RHA) suspension, aerated with recycled aluminium foil (A_R)

BA_R-RO: One-part eco-cellular concrete (ECC-OP) based on blast furnace slag (BFS) activated with olive-stone biomass ash/rice husk ash (OBA/RHA), aerated with recycled aluminium foil (AR) in which all the solid raw materials are co-milled and then blended with water (W).

2.1. Materials

Ordinary Portland cement (OPC: CEM I-52.5R) was supplied by Lafarge S.A (Puerto de Sagunto, Valencia, Spain), blast furnace slag (BFS) was acquired from Cementval S.A (Puerto de Sagunto, Valencia, Spain) as large granules. Olive stone biomass ash (OBA) was supplied by Almazara Candela (olive oil company, Elche, Spain). Rice husk ash (RHA) was supplied by DACSA S.A. (Tabernes Blanques, Valencia, Spain). The chemical compositions of these four materials were determined by X-Ray fluorescence (XRF, Magic Pro Spectrometer-Philips) and are summarised in Table 2.

Table 2. Chemical composition (XRF) of the raw materials (w%).

Material	Oxide composition (wt%)									
	SiO_2	CaO	Al_2O_3	Fe_2O_3	Na_2O	MgO	K_2O	P_2O_5	SO_3	Others	LOI*
OPC	20.80	65.60	4.60	4.80	0.07	1.20	1.00	-	1.70	-	0.23
BFS	30.53	40.15	10.55	1.29	0.87	7.43	0.57	0.26	1.93	0.89	5.53
RHA	85.58	1.83	0.25	0.21	-	0.5	3.39	0.67	0.26	0.32	6.99
OBA	5.33	27.77	0.70	3.45	0.78	5.13	32.12	2.68	1.67	1.47	18.90

*Loss on ignition

Commercial aluminium powder (A) was acquired from Schlenk Metallic Pigments GmbH and the recycled aluminium foil (A_R) was supplied by the Department of Agricultural Forest Ecosystems at the Universitat Politècnica de València (Valencia, Spain).

A milling treatment of the raw materials was required to manufacture alternative cellular concretes. A 1-litre capacity ball mill model Gabrielli Mill-2, with 98 alumina balls, was employed in all cases (except for RHA). The BFS used in the BA system was milled for 30 minutes and BFS+A_R was co-milled in the BA_R system. The RHA used in BA_R-R activation was singly pre-milled in an industrial grinder for 4 h (Bouzón et al., 2014). Finally, for the BA_R-RO samples, BFS, A_R, RHA and OBA were co-milled for 30 minutes and the obtained powder was employed as a single raw material in the ECC mix (one-part). The mean particle diameter (D_m) and particle size parameters (d(0.1) µm, d(0.5) µm and d(0.9) µm) were obtained with a Malvern Mastersizer 2000 laser granulometer in water suspension, and are summarised in Table 3.

Table 3. Mean particle diameter (D_m) and particle size parameters (d(0.1) µm, d(0.5) µm and d(0.9) µm) of the solid materials employed in cellular concretes.

MATERIAL	D_m (µm)	PARAMETERS		
		d(0.1)µm	d(0.5)µm	d(0.9)µm
BFS	28.8	2.8	19.7	68.9
BFS/A_R	29.3	2.8	19.9	70.2
RHA	20.3	2.5	10.5	41.2
BFS/A_R/RHA/OBA	25.1	1.2	14.5	66.4

The chemical reagents used for the alkali-activated solution preparation in AACCs (samples BA and BA_R) were sodium silicate (WG, 8 wt% Na_2O, 28 wt% SiO_2 and 64 wt% H_2O) and sodium hydroxide pellets (NaOH, 98% purity), both supplied by Merck-Spain.

2.2. Methods

2.2.1. Cellular concrete manufacturing

In this research, the volume of cellular concrete manufacturing was selected to obtain the material required to fill moulds for the functional features test (see the following section "2.2.2 Functional features"). For each batch, eight 1000-cm^3 cubes and six 64-cm^3 cubes were prepared.

The calculated dose for each sample is shown in Table 4. During the mixing procedure, the solid phase indicated the raw materials introduced as solid powders and the liquid phase corresponded to the added single materials (water in CA and BA$_R$-RO samples) or to the combined ones in aqueous medium (NaOH+WG alkali solution in BA and BA$_R$ or alternative OBA/RHA alkali suspension in BA$_R$-R).

Table 4. Doses (per mass) of the manufactured cellular concretes.

Sample	Solid phase	Liquid phase
CA	OPC: 7000.0 g A: 14.0 g	W: 3150.0 g
BA	BFS: 7000.0 g A: 14.0 g	W: 840.0 g NaOH: 426.8 g WG: 1968.8 g
BA$_R$	BFS: 7000.0 g A$_R$: 14.0 g	
BA$_R$-R	BFS: 7000.0 g A$_R$: 14.0 g	W: 3150.0 g NaOH: 945.0 g RHA: 918.8 g
BA$_R$-RO	BFS: 5600.0 g A$_R$: 16.8 g RHA: 716.7 g OBA: 2800 g	W: 3500.0 g

For samples CA, BA, BA$_R$ and BA$_R$-R, the liquid phase doses were determined according to previous works and experimental procedures (Font et al., 2018). For the new ECC-OP (BA$_R$-RO sample), the dose was determined based on the combination of previous ternary alkali-activated systems (BFS/RHA/OBA) with the addition of A$_R$ (Font et al., 2020). In this case, the water/solid ratio was selected by comparing several experimental parameters: the consistency of fresh pastes must be appropriate for developing a porous structure to avoid gas leaks through the matrix and to maximise gas entrapments in the matrix.

Mixing was carried out by a power drill, model AEG SBE705RE, connected to a paint mixer. The manufacturing procedure was divided into three stages, as shown in Table 5.

Table 5. Stages of the procedure carried out to manufacture each cellular concrete.

	PRE-MANUFACTURE	MANUFACTURE	POST-MANUFACTURE
CA	-	-**OPC/A** dry mix -**OPC/A** + **W** (180 s)	-24h (48h for BA_R-RO) RT[5] -Cut out the expanded free surface with a saw blade and demoulding. -RT until testing.
BA	-BFS grinding. -AS preparation[1]	-**BFS/A** dry mix -**AS** stirring (30 s) -**BFS/A+ AS** (180 s)	
BA_R	-BFS /A_R Co-milling -AS[1] preparation[2]	-**AS** stirring (30 s) -**BFS/A_R** + **AS** (180 s)	
BA_R-R	-BFS /A_R Co-milling -AAS[3] preparation[4]	-**AAS** stirring (30 s) -**BFS/A_R** + **AAS** (180 s)	
BA_R-RO	-BFS/A_R/RHA/OBA Co-milling	-**BFS/A_R/RHA/OBA** + **W**(180 s)	

[1]AS = alkali solution

[2]AS preparation: remained in a plastic beaker sealed with plastic film until room temperature was reached

[3]AAS = alternative alkali dissolution

[4]AAS preparation: NaOH pellets were dissolved in water by rising the temperature. Then RHA was added to the hot solution and mixed for 1 minute. The alternative alkali suspension was stored at 65ºC for 24 h to improve the silica solubilisation from RHA.

[5]RT = room temperature (23ºC/100% RH)

2.2.2. Functional features

The analysed functional features were density, compressive strength and thermal conductivity, according to the guidelines of Standard UNE EN 771-4: "*Specifications for masonry units-part 4: autoclaved aerated concrete masonry units*" (AENOR, 2016a) and compared to the ACI Committee 523.2-R96: "*Guide for Precast Cellular Concrete*" (Babbitt et al., 2014). The functional features tests were carried out after 28 curing days at room temperature (23ºC/100 RH).

A. DENSITY: Six specimens (4 x 4 x 4 cm^3) were employed to analyse the bulk and dry densities based on Standard UNE EN 772-13: *"Methods of test for masonry units-part 13: determination of net and gross dry density of masonry units (except for natural stone)"*(AENOR, 2001). Hydric tests were carried out as follows:

1. Dry weight (W_d) determination: specimens drying at 105±5 ºC until constant mass (24 h with a change in weight under 0.2%).
2. Absolute volume (or net volume) (V_n) of specimens obtained by hydrostatic balance means according to the specifications in UNE-EN 772-13 and by applying Equation (1):

$$V_n = \frac{W_a - W_w}{\rho_w} \; (m^3) \qquad (1)$$

Where:

V_n = Absolute volume (m^3).
W_a = Air weight of specimens (conditioning 2 h after the curing treatment under laboratory conditions) (kg).
W_w = Weight submerged in water (kg).
ρ_w = Water density (kg/m^3).

3. Absolute density (ρ_n) (or net density) calculation by Equation (2), as follows:

$$\rho_n = \frac{W_d}{(V_n - V_v)}\left(\frac{kg}{m^3}\right) \quad (2)$$

Where:
ρ_n = Dry density (kg/m^3).
W_d = Dry weight (kg).
V_n = Absolute volume (m^3).
V_v = Void volume (V_v = V_g - V_n, being V_g = gross volume), (m^3).

4. Bulk density (ρ_b) (or gross density) calculation by using Equation (3) as follows:

$$\rho_b = \frac{W_d}{(V_g - V_v)}\left(\frac{kg}{m^3}\right) \quad (3)$$

Where:
ρ_b = Bulk density (kg/m^3).
W_d = Dry weight (kg).
V_g = Gross volume (m^3).
V_v = Void volume (m^3).

B. COMPRESSIVE STRENGTH: Eight specimens (10 x 10 x 10 cm^3) were tested for the compressive strength (R_c) assessment, and the average and standard deviations were calculated. Standard UNE EN 772-1: "*Methods of test for masonry units-part 1: determination of compressive strength*"(AENOR, 2016b), was followed and a universal testing INSTRON 3282 machine was employed (see Fig. 2a) . The required loading rate (0.05 MPa per second) was adjusted at a displacement rate of 1 mm per minute. Samples were weighed before testing and natural density (ρ) was determined as the mass per unit volume.

C. THERMAL CONDUCTIVITY: Four samples (10 x 10 x 10 cm^3) were employed for thermal conductivity (λ) determinations according to Standard UNE EN 1745: *"Masonry and masonry products - methods for determining thermal properties"*(AENOR, 2013). For the test, a KD2-Pro handheld device (Decagon Devices Inc.) was used with a thick single RK-1 sensor (length x diameter = 6 cm x 0.39 cm) (see Fig. 2b). The measurement method was the transient line source, based on the dual needle probe system following ASTM D5534-08 (ASTM International, 2008) and IEEE 442-1981(IEEE STANDARDS ASSOCIATION, 1981). To accommodate the sensor, five distributed pilot holes (length x diameter = 6 cm x 0.4 cm) were drilled on the specimen surface.

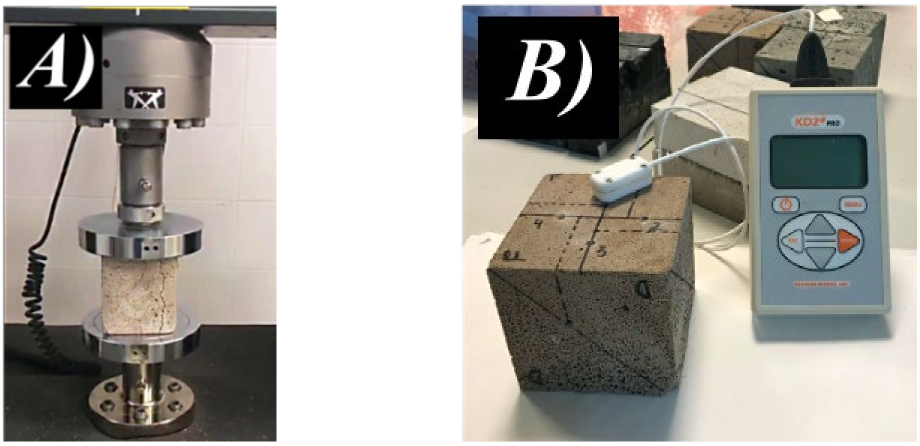

Fig. 2: Overview of dynamic testing performance: a) compressive strength; and b) thermal conductivity.

2.2.3. Life cycle assessment (LCA)

The cradle-to-gate modality of the LCA was selected to limit the study coverage by following Standard ISO 14040 and the Intergovernmental Panel on Climate Change 2006 (IPCC) specifications (IPCC, 2006). The manufacture of 1 m^3 of each proposed cellular concrete was analysed and compared (TCC, AACC, ECC and ECC-OP systems) in terms of their 100-years Global Warming Potential time horizon (100-GWP) associated with their materials and procedures. 100-GWP is a measure of how much heat the emissions of 1 ton of greenhouse gases will be trapped over a 100-year period in relation to the emissions of 1 ton of carbon dioxide (CO_2). Calculations were done from the extracted raw materials to their industrial block manufacturing, and before their distribution. Fig. 3 shows a correlational framework of the selected flows and processes from the studied "cradle-to-gate LCA" for manufacturing the masonry units of each material.

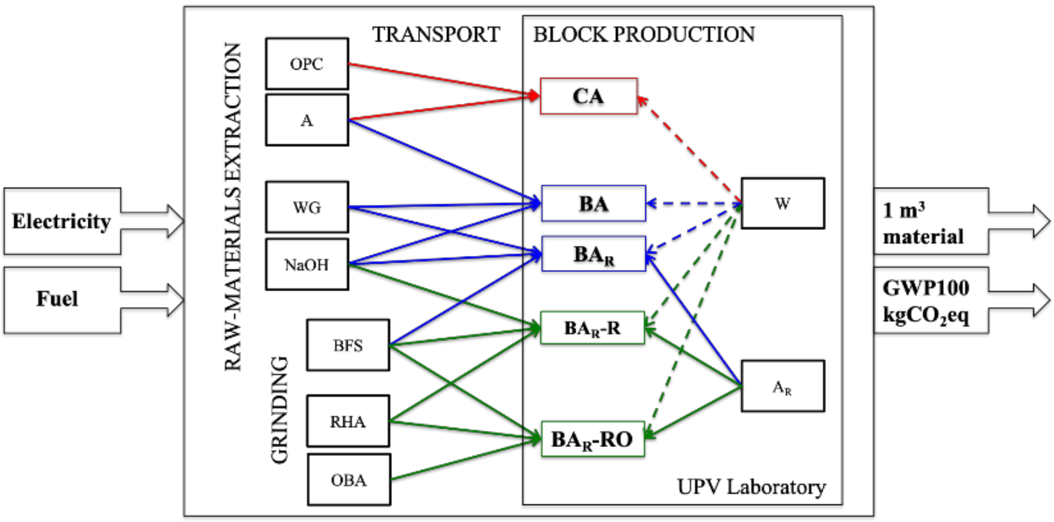

Fig. 3: Overview of the selected flows and processes in the cradle-to-gate LCA carried out to compare the industrial pre-cast blocks manufacturing with CA, BA, BA$_R$, BA$_R$-R and BA$_R$-RB.

The following considerations were taken for the LCA calculations:

- The industrial manufacturing of masonry units was selected, with dimensions 20x62.5x25 cm^3 and a density of 550 kg/m^3, by comparing the use of CA, BA, BA_R, BA_R-R and BA_R-RO. The 1 m^3 dose of each material was theoretically calculated with which 32 precast blocks could be manufactured. The European emission factors of manufacturing and equipment of this process are standardized in Ecoinvent 3.3. The curing treatment was not considered because the ambient temperature was selected for comparing the five cellular concretes. To reference the factory's location, the laboratory in the Universitat Politècnica de València (UPV) was selected.
- The proportion of the different materials was obtained using a thermogravimetric analysis (TGA) following the methodology introduced by Font et al. (Font et al., 2018). The TGA was carried out with a TGA 850 Mettler Toledo thermobalance within the 35-600ºC temperature range, in an N_2 atmosphere, and dry samples were placed inside aluminium crucibles with a micro-hole in their sealed lids. The weight loss obtained in the derivate thermogravimetric curves (DTG) was from the combined water. The constant range between the total solid weight and solid phases (precursor and from the alkali solution, Na_2O and SiO_2) in the cellular concretes was employed to obtain the doses of the theoretical samples for the LCA.
- BFS was considered a by-product as suggested by Van Der Heede and De Belie (Van Den Heede and De Belie, 2012) and Chen et al.(Chen et al., 2018). Their secondary production includes treatment and refurbishment after metal collection: solidification (granulated BFS) and grinding (BFS). As RHA and OBA were wastes, their extraction was not considered, but their necessary conditioning pre-treatment was taken into account to be employed in cellular concrete manufacturing.
- The milling treatment of all the alternative raw materials was considered and was carried out the same as the milling treatment for OPC (equipment and energy demands) in the Cementval S.A industrial plant (Puerto de Sagunto, Spain).
- The used transport references were: Diesel truck, EURO4, ≤ 7.5t and mixed transport (urban/interurban). Distances were selected from the raw-materials extraction emplacements to the UPV laboratory as the sum of the lorry's return trips (British Standards Institution, 2011) (see Table 5). If two raw materials came from the same company, only one transport unit was considered (with length taken as only the sum of the two raw materials without it exceeding the lorry's capacity).
- In the production unit for BA_R-R, the alkali suspension preparation was included in the calculations by considering the more extreme situation: two electric resistances of 1 kW operating for 24 h to keep water at 65ºC (by assuming that the water in the bath was hot at the time the alkali solution was being prepared).

The software employed to perform the analysis was OpenLCA 1.7.2 with a combination of life-cycle inventory (LCI) databases from Ecoinvent 3.3 Open LCA Nexus

(Ecoinvent Association, 2019; Moreno-Ruiz E. et al., 2019). Table 6 provides the employed LCI and the corresponding environmental emission factors (EF) for each unity, as well as transport distances (km).

Table 6. Employed LCI, environmental emission factors (EF) for each unity and transport distances (km)

		EF	**LCI**	**Distance**[1]
Raw materials	OPC	0.907 $kgCO_2eq$ / kg	Ecoinvent[4]	53.8 km
	BFS	0.0192 $kgCO_2eq$ / kg	Ecoinvent[4]	53.4 km
	A	15.601 $kgCO_2eq$ / kg	Ecoinvent[4]	710 km
	A_R	0	-	0 km
	NaOH	1.120 $kgCO_2eq$ / kg	SimaPro[5]	732 km
	WG	1.213 $kgCO_2eq$ / kg	SimaPro[5]	
	RHA	0	-	53.4 km
	OBA	0	-	
Water (W)		4.288 x 10^{-4} $kgCO_2eq$ / kg	Ecoinvent[4]	0 km
Transport		0.126 $kgCO_2eq$ / km	(IDAE, 2019)	
Grinding	Power	35.4 kWh / ton		
	Energy[2]	0.272 $kgCO_2eq$ / kWh		
Production	Thermal bath[3]	0.272 $kgCO_2eq$ / 2 kW * 24 h	(CNMC, 2018)	
	Manufacture	0.138 $kgCO_2eq$ / block	Ecoinvent[4]	

[1] Sum of return lorry routes from the extraction emplacement to the UPV laboratory.
[2] National Energy Mix (2018)
[3] In the BA_R-R alkali solution preparation: two electrical resistances working for 24 h.
[4] http://www.openlca.org/ecoinvent-3-3-released-in-openlca-nexus/
[5] https://simapro.com/licences/#/business

3. Results and Discussion

In the Fig. 4 some pictures (10 cm size cubic specimens) of the TCC (CA specimens), the AACC with A_R co-milled with the BFS as aerating agent (BA_R specimens) and the ECC-OP (BA_R-RO specimens) obtained are shown, where a different colour and porous-structure appearance can be observed among the concretes.

Fig. 4: Pictures of the visual appearance of the obtained materials (10 cm cubic specimens): a) Traditional celular concrete (CA sample); b) Alkali activated cellular concrete (BA_R sample); and c) One-part eco-cellular concrete (BA_R-RO sample).

3.1. Functional features

European standard in UNE-EN UNE EN 771-4 sets a maximum bulk density of 1,000 kg/m^3 and a minimum compressive strength of 1.5 MPa for autoclaved aerated concrete masonry unit applications. The reference values set by the ACI Committee 523.2-R96, "*Guide for Precast Cellular Concrete*", are a maximum bulk density of 800 kg/m^3 and a minimum compressive strength of 2.07 MPa for applications to floor, roof and wall units.

Table 7 provides the results of the hydric (absolute density (ρ_n) and bulk density (ρ_b)) and physical/mechanical (natural density (ρ) and compressive strength (R_c)) tests.

Table 7. Results of the hydric and mechanical tests for the studied cellular concretes after 28 days.

Sample	Hydric tests		Mechanical tests	
	ρ_n (kg/m^3)	ρ_b (kg/m^3)	ρ (kg/m^3)	R_c (MPa)
CA	661 ± 6	617 ± 9	618 ± 2	6.5 ± 0.4
BA	770 ± 1	635 ± 3	583 ± 4	6.1 ± 0.2
BA_R	778 ± 7	681 ± 8	674 ± 4	7.1 ± 0.2
BA_R-R	794 ± 8	616 ± 2	691 ± 4	5.6 ± 0.3
BA_R-RO	713 ± 1	660 ± 8	704 ± 4	6.3 ± 0.1

As expected, the bulk density and compressive strength values of the CA samples (TCC) fell well within the mandated requirements of UNE EN 771-4 and the ACI Committee 523.2-R96. The TCC systems yielded 617 kg/m^3 for bulk density and 618 kg/m^3 as natural density with 6.5 MPa after 28 curing days under ambient conditions.

In general, the studied alternative cellular concretes yielded similar absolute and bulk densities to the TCC ones. In the first step of the greener improvements in cellular concretes (BA sample), when the alkali-activated slag replaced the use of OPC, the obtained values of absolute and bulk densities were slightly higher than for the TCC mix (CA), 14% for ρ_n and 3% for ρ_b. In the second step (the second AACC system), when commercial A was replaced with recycled foil (BA_R sample), the increase in ρ_n and ρ_b was 14% and 8%, respectively. The next improvement introduced into the systems gave way to the first ECC (BA_R-R), in which the silica source resulted from using RHA. This sample achieved an absolute density that was 17% higher than the TCC samples, but bulk density was similar (617 kg/m^3 for the CA sample vs. 616 kg/m^3 for the alternative BA_R-R sample). Finally, the ECC-OP made from 100% residues (BA_R-RO sample) achieved an absolute density that was 7% higher and a bulk density that was 6% higher than the control TCC.

Regarding the natural density and compressive strength of the alternative cellular concretes, when the alkali-activated technology was introduced (AACC systems) and the material was aerated by A, the BA sample yielded 583 kg/m^3 and 6.1 MPa after 28 curing days at room temperature. Similar systems with alkali-activated slag aerated with commercial aluminium powder have been studied by Esmaily and Nuranian, who presented 1,227 kg/m^3 and <1 MPa at curing regime temperatures for 14 h (Esmaily and Nuranian, 2012). When the second step was introduced and the aluminium powder source was replaced with recycled foil (the BA_R sample), natural density was higher (674 kg/m^3) and compressive strength increased by 1 MPa (compared to the previous AACC system, the BA sample).

The ECC system (the BA_R-R sample) yielded 691 kg/m^3 and 5.6 MPa. The introduction of RHA as a silica source into the replacement of sodium silicate allowed the natural density range to be maintained, but compressive strength slightly decreased (BA_R-R vs BA_R). In previous research works, the same systems were developed and compared, and the only difference was the water/binder (w/b) ratio (Font et al., 2018): i) for the previous AACC (BFS + A_R + ordinary alkali solution (WG + NaOH + W)), the w/b ratio was 0.35 (the w/b ratio herein was 0.30); ii) in the previous ECC (BFS + A_R + alternative alkali solution (RHA + NaOH + W)), the w/b ratio was 0.45 (the w/b employed was 0.40 herein). These previous results showed that density increased from 474 kg/m^3 to 611 kg/m^3 when commercial waterglass was replaced with RHA, and compressive strength also increased from 2.6 MPa to 4.6 MPa after 28 curing days at room temperature. A lower w/b ratio allowed an increase in viscosity, which was enough to void/system development with a stable matrix yielding higher density (but < 1,000 kg/m^3) and greater compressive strength. This influence was much stronger for the AACC systems than for the GCC ones.

Finally, the one-part eco-cellular concrete (BA_R-RO) sample, where sodium silicate was replaced with OBA, yielded 704 kg/m^3 and 6.3 MPa. The first 100% waste-based one-part eco-cellular concrete increased density by less than 100 kg/m^3 and merely decreased 0.1 MPa compared to the TCC manufactured under the same conditions.

To analyse the evolution of the natural density and compressive strength achieved with the step-by-step greener improvements, a relative coefficient can be obtained by taking the TCC system values as a reference:

$$\varphi_d = {\rho_A}/{\rho_r} \tag{4}$$

Where:
φ_d = Density relative coefficient
ρ_A = Natural density of the selected alternative cellular concrete (kg/m^3)
ρ_r = Natural density of the reference cellular concrete (the CA sample) (kg/m^3)

$$\varphi_R = {}^{R_A}/_{R_r} \tag{5}$$

Where:
φ_R = Compressive strength relative coefficient
R_A = Compressive strength of the selected alternative cellular concrete (MPa)
R_r = Compressive strength of the reference cellular concrete (the CA sample) (MPa)

The coefficients near the unity indicated a close relation between the materials (alternative with reference cellular concretes).

Relative factor ω, obtained by the ratio between the relative coefficients of the natural density and compressive strength, can be obtained with these relative values:

$$\omega = \varphi_d/\varphi_R \tag{6}$$

Where:
ω = Relative factor between density and compressive strength
φ_d = Density relative coefficient
φ_R = Compressive strength relative coefficient

In this case, relative factor (ω) equalled the unity, which indicated that the material presented an equal relationship between density and compressive strength as CA.

The Fig. 5 shows the obtained coefficients (φ_d and φ_R) and the relative factor (ω) for the alternative cellular concretes.

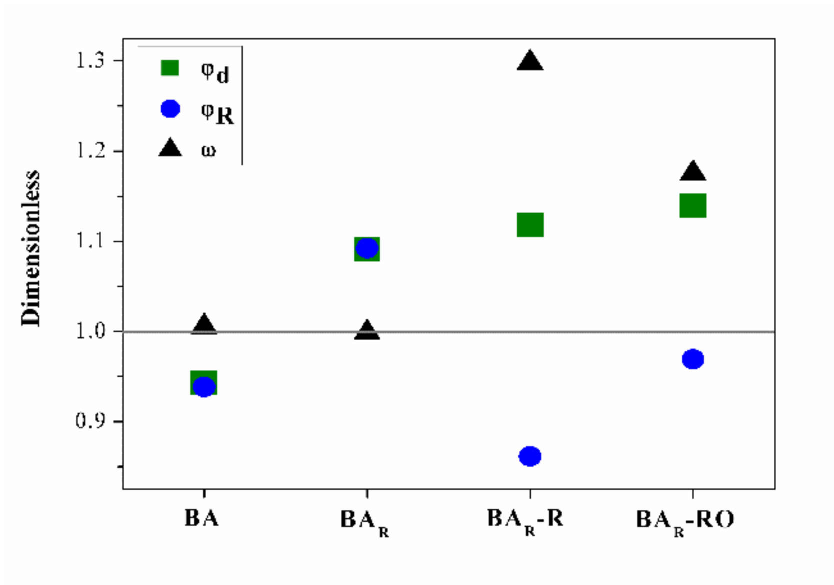

Fig. 5: The relative coefficients of density (φ_d) and compressive strength (φ_R)) and relative factor (ω) for the alternative cellular concretes

As observed, both coefficients were below the unit line for the BA sample, which indicates that the density and the compressive strength values are less than those of the CA samples. The overlapping of coefficients φ_d and φ_R indicates the direct linear relation between density and compressive. For the BA_R sample, where alternative aluminium was employed as an aerating agent, the φ_d and φ_R values were above the unit line.

When RHA was employed as a silica source (BA$_R$-R sample), the coefficients were above the unit line for density and below it for compressive strength, which indicates an inverse relation of the obtained properties vs. the control (CA). The same behaviour was observed for the proposed ECC-OP, where OBA was employed as an alkali source to avoid chemical reagents: the BA$_R$-RO sample allowed greater mechanical behaviour to be achieved with less commitment to density.

When observing the resultant relative factor for the two AACC samples (BA and BA$_R$), which were on the unit line in the graph, it was established that the relation between the two properties was similar to the control one. With the ECC samples (BA$_R$-R and BA$_R$-RO), the relation between the properties when comparing it to the control was greater than the unit, and the new BA$_R$-RO relative factor came nearest to the unit. This reveals that with a determined compressive strength value, the ECC-OP system aerating effect was less than for the ECC system. As alkalinity provided by OBA in the systems, it was is less than that provided by NaOH, the reaction rate and, consequently, hydrogen generation were lower for the ECC-OP systems.

It is highlighted that the standard specification was substantially exceeded by all the alternative developed cellular concretes, as shown in Fig. 6. In bulk density terms (Fig. 6b), the improvement of BA$_R$-RO can be established as a lower percentage in relation to: i) UNE EN 771-4 (1,000 kg/m^3) with 34%; and ii) the ACI Committee 523.2-R96 (800 kg/m^3) with 18%. For compressive strength (Fig. 6b), the improvement for BA$_R$-RO was represented by an increased percentage as follows in relation to: i) UNE EN 771-4 (1.5 MPa) with 320% (an increase of 4.8 MPa); and ii) the ACI Committee 523.2-R96 (2.07 MPa) with 204% (an increase of 4.2 MPa).

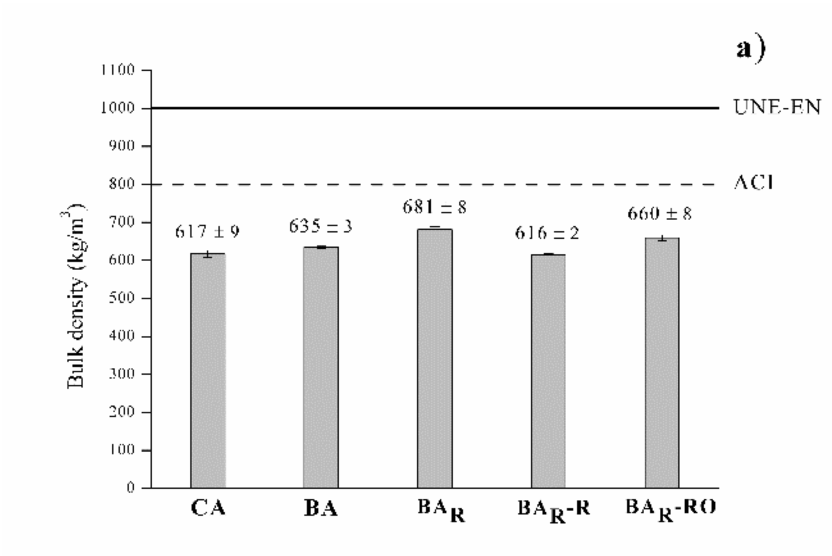

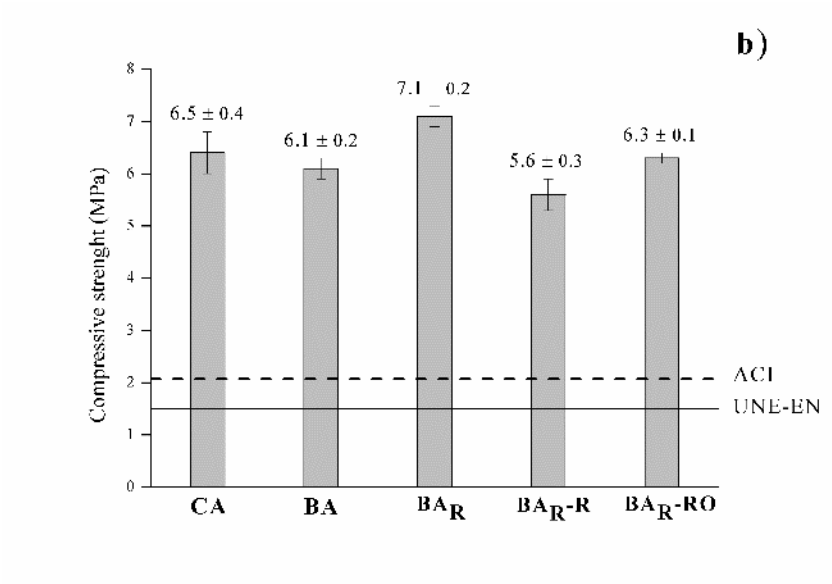

Fig. 6: a) Bulk densities obtained after 28 days and the lines of the maximum limited values by standards UNE-EN and ACI; b) compressive strength after 28 days and the lines of the minimum limited values by standards UNE-EN and ACI.

According to the catalogue of building elements established by the Technical Building Code (CTE) (Ministerio de Fomento - Gobierno de España, 2018), autoclaved aerated concrete masonry units should meet thermal property requirements according to their bulk density. These ratios are proposed to fulfil general design requirements in habitability demands, and in energy efficiency and energy saving plan terms. The same ratio between bulk density and required thermal conductivity is proposed by ACI committee 523.2R-96 (Babbitt et al., 2014).

The maximum thermal conductivity value and its dependence on bulk density (CTE and ACI requirements) are shown in Table 8, which were compared to the experimental values obtained for the studied cellular concretes.

Table 8. Thermal conductivity of the analysed cellular concretes: values obtained in the study and the CTE/ACI requirements based on bulk density.

	Obtained values		CTE		ACI	
Sample	ρ_b (kg/m^3)	λ (W/mK)	ρ_b (kg/m^3)	λ (W/mK)	ρ_b (kg/m^3)	λ (W/mK)
CA	617 ± 9	0.18 ± 0.01	600	0.18	640	0.20
BA	635 ± 3	0.13 ± 0.02	600	0.18	640	0.20
BA$_R$	681 ± 8	0.28 ± 0.07	700	0.20	640	0.20
BA$_R$-R	616 ± 2	0.22 ± 0.01	600	0.18	640	0.20
BA$_R$-RO	660 ± 8	0.20 ± 0.01	700	0.20	640	0.20

As observed, the required insulation values were achieved by TCC (the CA sample), and also by the resulting material in the first step towards greener improvements (when the alkali-activated technology was applied), namely the BA sample (the first AACC system). The thermal conductivity of the BA (0.13 W/mK) sample was lower than it was for the CA sample (0.18 W/mK), which indicates greater insulation properties. When addressing the second step, and the commercial aluminium powder was replaced with recycled foil milled by the precursor (the BA_R sample), thermal conductivity (0.28 W/mK) was higher than that required by the standards UNE-EN (0.20 W/mK) and by ACI (0.18 W/mK). This second AACC system was the less insulating one of all the studied materials. When RHA was used as a silica source (ECC, the BA_R-R sample) the thermal insulation properties were enhanced (λ = 0.22 W/mK), but this was not enough to fulfil the standards. The BA_R-RO sample (the ECC-OP system) yielded a thermal conductivity value within the limits of both standards (0.20 W/mK), which indicates enhanced improvement in the material's thermal insulation properties when adopting 100% greener alternatives in the dose.

3.2. Live cycle assessment (LCA)

The LCA was performed based on the conditions of the experimental samples followed in this investigation, especially considering that all the samples were cured at room temperature. Table 9 shows the TGA results for the different assessed pastes and the calculated proportions of the materials for the LCA. These proportions allowed 1 m^3 to be obtained for each proposed material to manufacture 32 pre-cast blocks with a density of 550 kg/m^3.

Table 9. The total weight loss (TWL %) obtained in the TGA test and the theoretical calculated proportion (in mass) for manufacturing 1m^3 (32 pre-cast blocks) for each cellular concrete.

Sample	TWL %	Solid phase (kg)	Liquid phase (kg)
CA	17.57	OPC: 453.3 (69 %)[1] A: 0.9 (1 %)	W: 204.0 (30 %)
BA	13.45	BFS: 414.5 (68 %) A: 0.8 (1 %)	W: 49.7 (3 %) NaOH: 25.3 (8 %) WG: 116.6 (20 %)
BA_R	13.60	BFS: 413.8 (68 %) A_R: 0.8 (1 %)	W: 49.5 (3 %) NaOH: 25.2 (8 %) WG: 116.4 (20 %)
BA_R-R	12.60	BFS: 393.1 (58 %) A_R: 0.8 (1 %)	W: 177.0 (26 %) NaOH: 53.1 (8 %) RHA: 51.6 (7 %)
BA_R-RO	11.50	BFS: 323.8 (44 %) A_R: 1.2 (1 %) RHA: 41.4 (5 %) OBA: 161.9 (22 %)	W: 202.4 (28 %)

[1] In brackets: percentage representing the raw material vs. the total proportion of cellular concrete.

The resulting matrices of the $kgCO_2eq$ from the different flows and the total 100-GWP for the CA, BA, BA_R, BA_R-R and BA_R-RO cellular concrete systems are plotted from Fig. 7 to Fig. 11, respectively.

The raw materials extraction had the strongest impact on CA utilisation and represents 81% of the total emissions. In the TCC material, OPC had the strongest influence on dose (69%) but its influence was stronger on the total 100-GWP (96%) compared to the other materials (A and W). The pre-treatment of the raw materials (grinding) was not included because it was carried out on both the primary OPC and primary A industrial procurements (extraction). Despite the low dose of A in the CA manufacturing (0.2% of the OPC weight, which represents a 0.13% dose of the total CA components), its extraction substantially impacted the LCA (14% of the total 100-GWP). Transport activity led to 18% of the total 100-GWP. Thus the distance from the company which supplied the UPV laboratory with A was the longest (see Table 6): the A in this flow was the most influential greenhouse gas producer (93%). The production of 1m^3 (standardised European equipment and block manufacture procedures) had the least influence on the total environmental impact (1% of the total 100-GWP).

The masonry unit manufacturing performed by the TCC system technology yielded a 100-GWP of 526 kgCO_2eq. This value was slightly higher than that presented by Yang et al (Yang et al., 2014), who indicated a 1 m^3 production of 500-kg/m^3 OPC-based foamed concrete that yielded 412 kgCO_2eq. Those authors considered only the go-trip in the transport flows and the material's lower density. Thus their lower OPC dose could cause this reduction. Dahmen et al (Dahmen et al., 2018) recently assessed the life cycle of OPC-based masonry blocks and obtained 216 kgCO_2eq by using 1,840-kg/m^3 materials. However, these blocks had a 66% higher volume than the cellular concrete herein analysed, where OPC was only 11% of the concrete dose in this manufacturing.

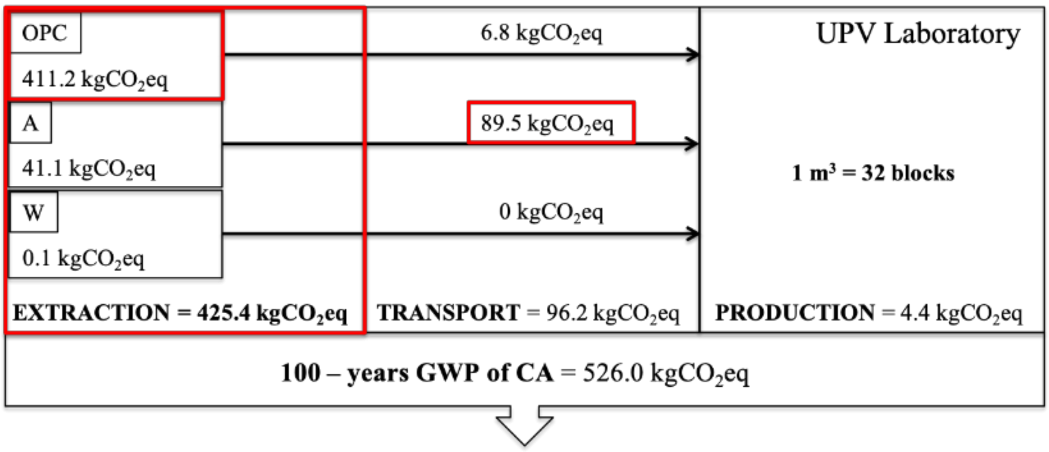

Fig. 7: The 100-GWP impacts associated with each unitary flow and the production of 1m^3 of CA (in red, the unit or subunit with the strongest influence).

With the first step environmental improvement (the BA samples), the influence of raw materials extraction dropped by 56% and represented 49% of the total 100-GWP. The highest dose material was BFS, but WG was the most influential component on environmental impact emissions. Relative to the dose total materials, the proportion of BFS was 68 % and the proportion of WG was 20 %, however, in terms of 100-years GWP, the influence of BFS was merely 4 % and the influence of WG was 74 %. The key role of WG on the AAM environmental impact is commonly found (Mellado et al., 2014; Moraes et al., 2018; Puertas and Torres-Carrasco, 2014). As the influence of BFS grinding was introduced into the LCA calculations in that step, the improvement compared with OPC extraction offset emissions (the sum of BFS extraction and grinding was 55% lower than it was for OPC production). Transport flow was higher than the CA sample because the needed commercial chemical activators (WG and NaOH) and this influenced negatively in the total GWP improvements. For manufacturing BA blocks, the influence of transport was 49% because total emissions were the main cause from transporting the required chemical reagents and A (49% and 47%, respectively). The production process of the masonry units was maintained constant as it was the same for both materials and continued to be the lowest flow.

The masonry unit manufacturing done with the BA cellular concretes (the AACCs technology) yielded 386 kgCO_2eq of the total 100-GWP. This value was 27% lower than the CA material. When considering the drastic reduction in the material volume of required material when using cellular concretes, and the good performance of previously studied functional requirements, the results in the ACV of BA can be compared with the traditional systems found in the bibliography. Robayo-salazar et al. (Robayo-salazar et al., 2018) compared the GWP of compounds of natural pozzolan/BFS in 70/30 proportions with the OPC ones to find a 45% reduction in total emissions. The works published about BFS-cellular concretes Yang et al. present reductions up to 85% compared to OPC cellular concretes (Yang et al., 2014). As explained above, those authors only considered one transport trip and the considered doses were lower than those analysed in the present work.

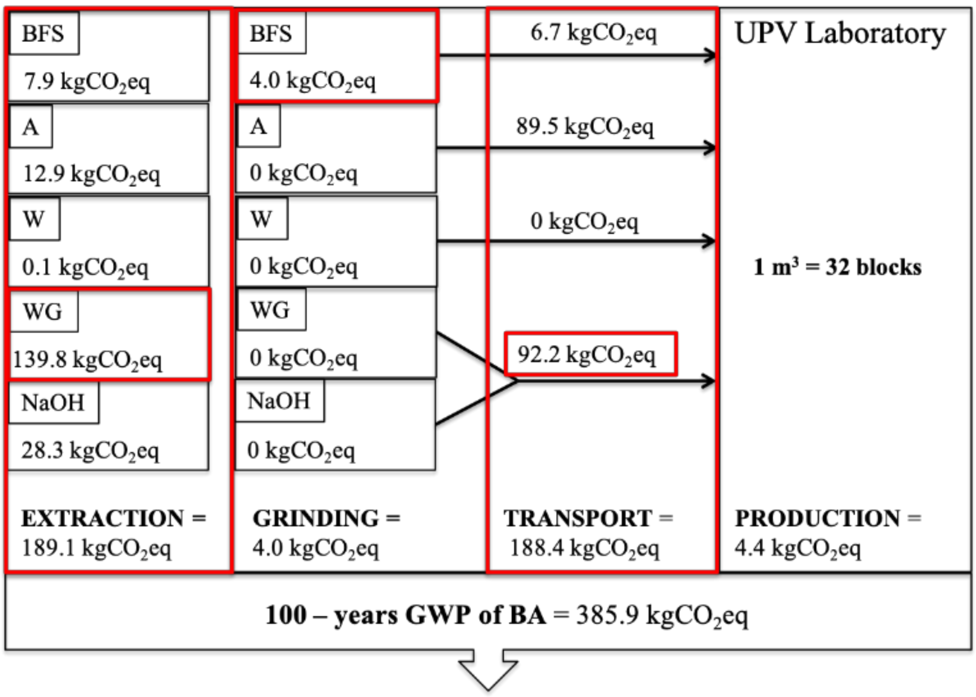

Fig. 8: The 100-GWP impacts associated with each unitary flow and a total production of 1m^3 of BA (in red, the unit or subunit with the strongest influence).

By replacing commercial A with recycled foil (the BA_R material), a total 27% 100-GWP improvement was achieved. However, the most marked decrease was found in transport flow (47% lower than BA) as A_R was not considered because it was obtained directly from the UPV laboratories. Material extraction decreased by 7%, and grinding and production flows remained constant.

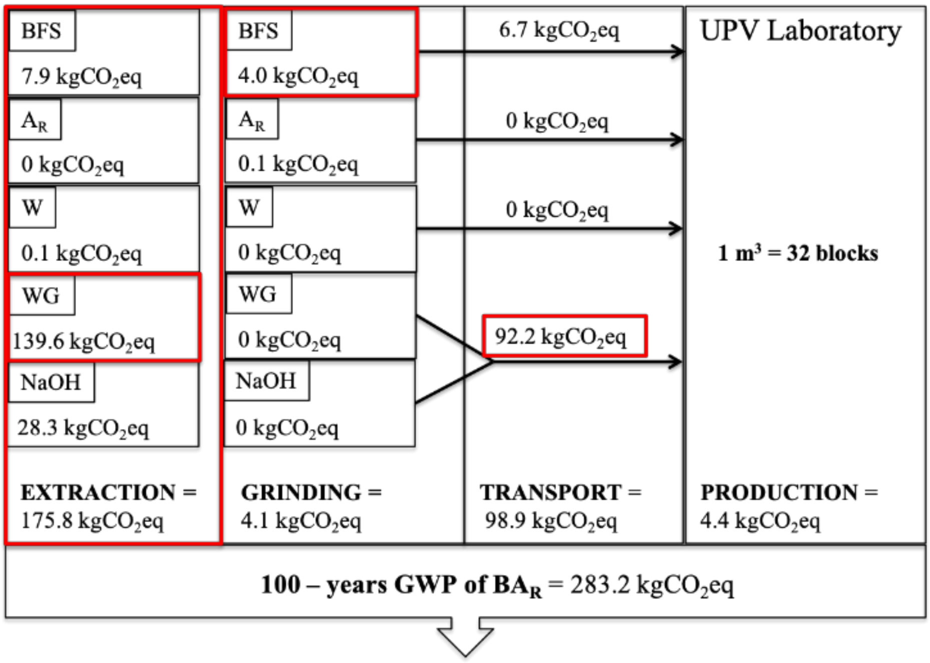

Fig. 9: The 100-GWP impacts associated with each unitary flow and a total production of 1m^3 of BA_R (in red, the unit or subunit with the strongest influence).

The ECC system (when using RHA as a silica source) allowed a 36% improvement in the 100-GWP compared to the BA_R sample and one of 66% vs. CA. Mellado et al. (Mellado et al., 2014) found that CO_2 emissions reduced by 50% when WG was replaced with RHA in the alkali activator dissolution for FCC-based mortars manufacturing. The improvement in the material herein developed allows an 80% reduction in the material's volume. By using BA_R-R, the emissions due to material extraction reduced by 62%. The strongest influence was NaOH, whose production released 59% of the total extraction flow. Transport flow was the same kgCO$_2$eq as the previous AACC system because the transport of NaOH had to still be considered. The introduction of RHA involved an increase in GWP for the raw materials pre-treatment requirements (grinding, 7% more than BA_R). Pre-cast block production required a 24-hour storage of the RHA/NaOH/water alkali solution, and the production flow increased by 60% at 24 h. With the use of BA_R-R the production flow was 10.9 kgCO$_2$eq versus the other studied materials with 4.4 kgCO$_2$eq. However, the total 100-GWP lowered thanks to the reduction in the other flows.

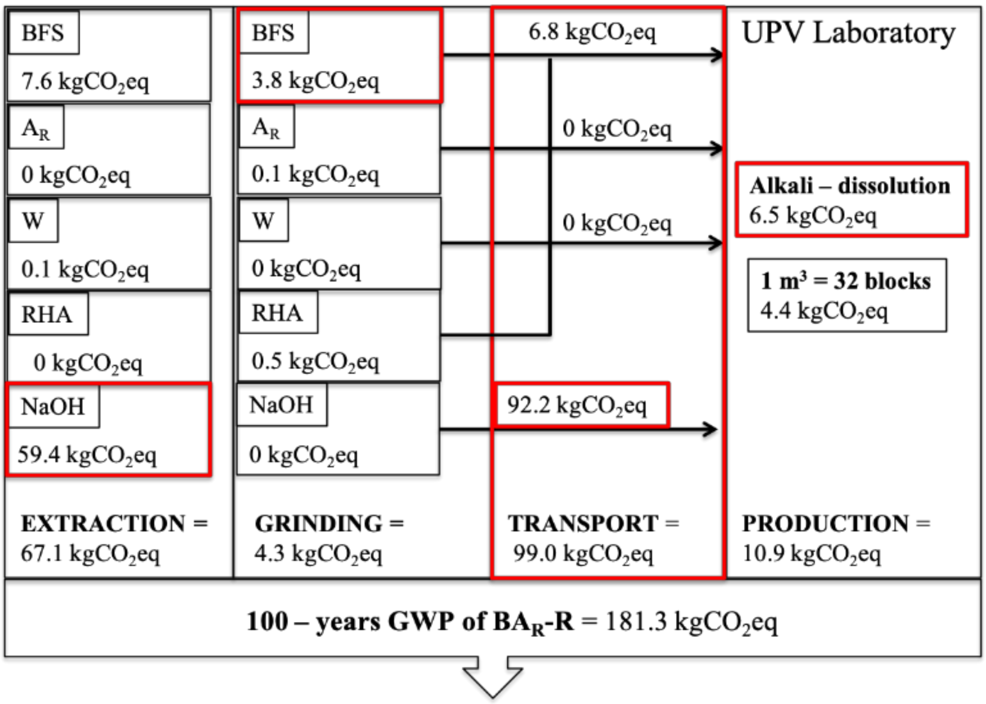

Fig. 10: The 100-GWP impacts associated with each unitary flow and to a total production of 1m^3 of BA_R-R (in red, the unit or subunit with the strongest influence).

Finally, with the one-part eco-cellular concrete, the total 100-GWP was 19 kgCO_2eq. The use of OBA as an alkali source allowed 100% waste-based material to be obtained, which was positively reflected by the environmental impact. It should be highlighted that the four processes had a proportional environmental impact with no flow with more than 10 kgCO_2eq (30% of total emissions).

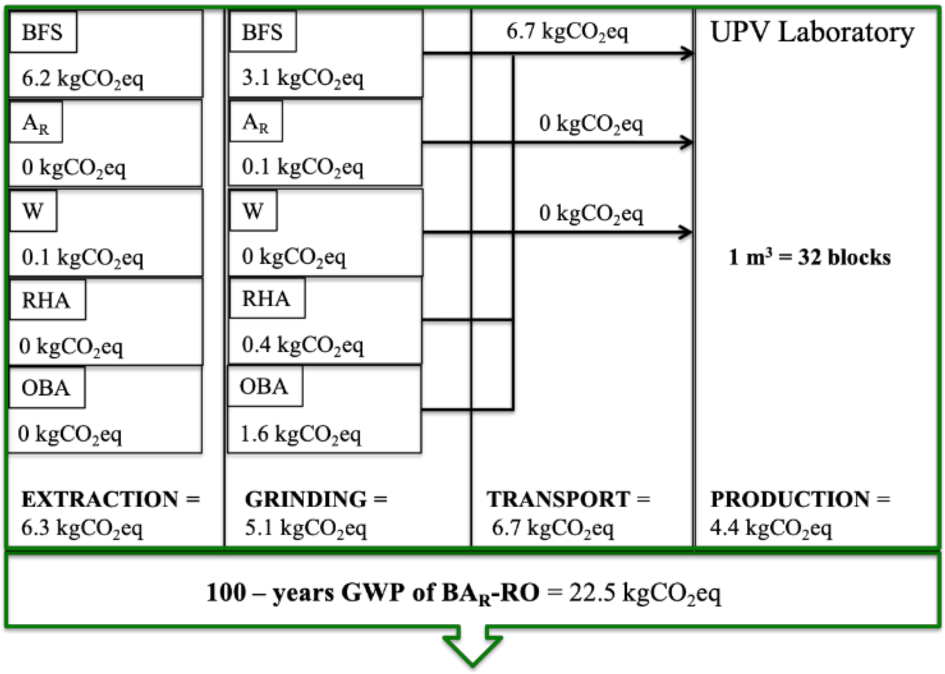

Fig. 11: The 100-GWP impacts associated with each unitary flow and a total production of 1m^3 of BA_R-RO (in red, the unit or subunit with the strongest influence).

The Fig. 12 shows the percentages of progressive decreases in the total 100-GWP achieved with each step-by-step greener improved material. The drawings inside each material-cloud show the influence of the different flows on the total 100-GWP. The new one-part 100% waste-based material, namely the ECC-OP system, yielded a total 96% reduction compared to TCC based on OPC (CA).

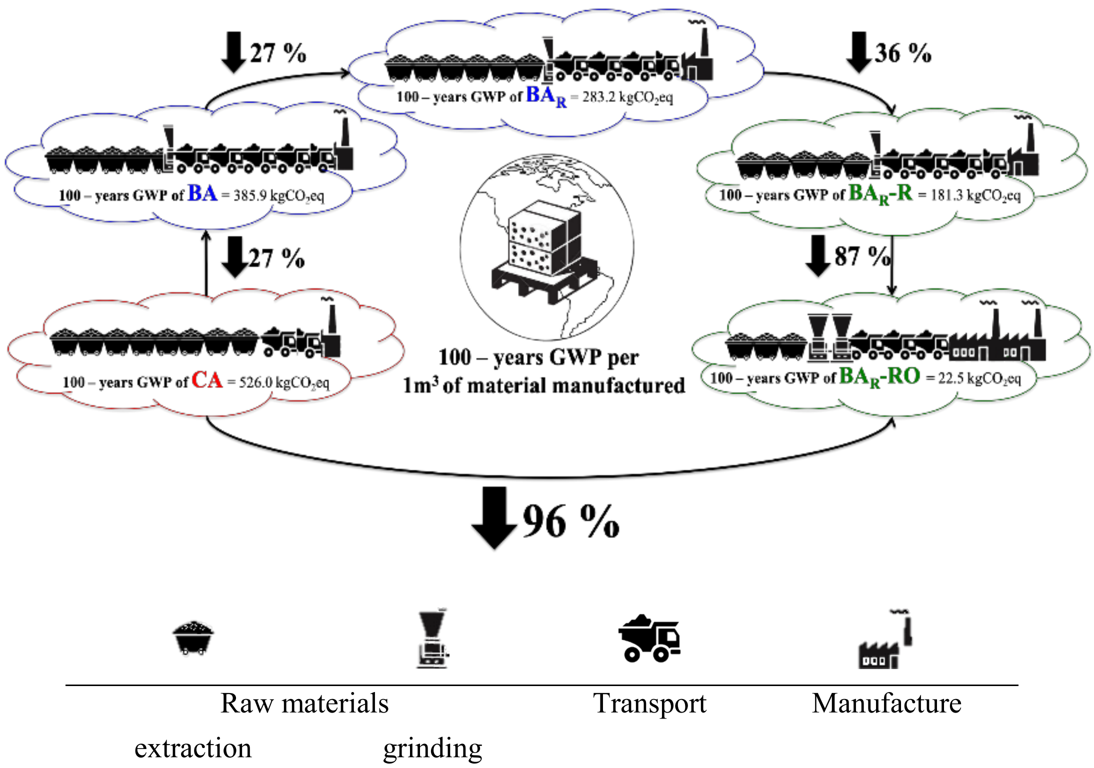

Fig. 12: Overview of total 100-GWP per 1m^3 of material manufactured and its progressive decreases with each step-by-step greener improvement introduced in the materials and manufacture.

4. Conclusions

The study of step-by-step greener improvements in the manufacturing of cellular concretes was successfully implemented.

The proposed alternative cellular concretes (the AACC, ECC and ECC-OP systems), yielded similar absolute and bulk densities to TCC. In the last step, a new one-part eco-cellular concrete was developed with only an increase in density of 100 kg/m^3 compared to CA, but compressive strength was similar to the traditional system.

This research presents an evaluation of functional features in line with European and American standards to apply cellular concrete to precast masonry units manufacturing:

- All the alternative developed cellular concretes well exceeded the obtained bulk density and compressive strength.
- For thermal conductivity, the required minimum value depends on the material's bulk density. Compared with standard specifications (CTE and ACI), the application of alkali activation technology (BA) yielded values that complied with those specified, but with the introduction of recycled foil (second step, the BA_R sample), as well as the silica-based residue (third step, the BA_R-R sample), the materials' thermal requirements were not met. Finally, the new 100% waste-based one-part eco-cellular concrete (ECC-OP) met the standard, and displayed a major eco-efficiency improvement for the alternative cellular concretes.

The acoustic insulation properties are close related to the thermal conductivity in cellular concretes. The total porosity, and its distribution into the matrix, will determine the acoustic insulation of the cellular concretes. The durability of cellular concretes is also related with the porosity and its size distribution. After careful consideration, it was verify the accomplishment of the new one-part ECC with functional features pursuant by the standards. A future experimental study will be developed on the porosity, acoustic properties and durability for the new cellular concrete.

The LCA done with the step-by-step greener improvements in the materials showed a progressive reduction in the 100-GWP ($kgCO_2eq$) compared to TCCs: 27% for BA, 46% for BA_R, 66% for BA_R-R and 96% for BA_R-RO.

This research shows the possible utilisation of the new ECC in precast masonry unit manufacturing. Its functional features comply with standards' specifications and its manufacturing by combining 100% waste-based and "one-part" technology concepts, which involves near-zero energy use and scarce greenhouse gas emissions.

Conflict of interest

None.

Acknowledgements

The authors gratefully acknowledge the GeocelPlus-UPV Project, Almazara Candela – Elche, Spain and DACSA S.A. - Tabernes Blanques, Spain and Cementval – Puerto de Sagunto, Spain.

References

AENOR, 2016a. UNE-EN 771-4:2011+A1: Especificaciones de piezas para fábrica de albañilería Parte4: Bloques de horigón celular curado en autoclave.

AENOR, 2016b. UNE-EN 772-1:2011+A1: Métodos de ensayo de piezas para fábrica de albañilería. Parte 1: Determinación de la resistencia a compresión.

AENOR, 2013. UNE-EN 1745: Fábrica de albañilería y componentes para fábrica. Métodos para determinar las propiedades térmicas.

AENOR, 2001. UNE-EN 772-13: Métodos de ensayo de piezas para fábrica de albañilería. Parte 13: Determinación de la densidad absoluta seca y de la densidad aparente seca de piezas para fábrica de albañilería (excepto piedra natural) 9.

ASTM International, 2008. ASTM D5334 - 14 Standard Test Method for Determination of Thermal Conductivity of Soil and Soft Rock by Thermal Needle Probe Procedure [WWW Document].

Babbitt, F., Barnett, R.E., Cornelius, M.L., Dye, B.T., Liotti, D.L., Schmidt, S.B., Tanner, J.E., Valentini, S.C., 2014. ACI 523.3R-14 Guide for Cellular Concretes above 50 lb/ft3 (800 kg/m3).

Bai, C., Colombo, P., 2018. Processing , properties and applications of highly porous geopolymers : A review. Ceram. Int. 44, 16103–16118. https://doi.org/10.1016/j.ceramint.2018.05.219

Bouzón, N., Payá, J., Borrachero, M. V., Soriano, L., Tashima, M.M., Monzó, J., 2014. Refluxed rice husk ash/NaOH suspension for preparing alkali activated binders. Mater. Lett. 115, 72–74. https://doi.org/10.1016/j.matlet.2013.10.001

British Standards Institution, 2011. PAS 2050:2011 Specification for the assessment of the life cycle greenhouse gas emissions of goods and services. London.

Chen, Y., Ko, M., Chang, J., Lin, C., 2018. Recycling of desulfurization slag for the production of autoclaved aerated concrete. Constr. Build. Mater. 158, 132–140. https://doi.org/10.1016/j.conbuildmat.2017.09.195

Chica, L., Alzate, A., 2019. Cellular concrete review: New trends for application in construction. Constr. Build. Mater. 200, 637–647. https://doi.org/10.1016/j.conbuildmat.2018.12.136

Choo, H., Lim, S., Lee, W., Lee, C., 2016. Compressive strength of one-part alkali activated fly ash using red mud as alkali supplier. Constr. Build. Mater. 125, 21–28. https://doi.org/10.1016/j.conbuildmat.2016.08.015

CNMC, 2018. Sede electrónica - Listado de Informes de Etiquetado de Electricidad [WWW Document]. Com. Nac. los Mercados y la Competencia. URL https://gdo.cnmc.es/CNE/resumenGdo.do?anio=2018 (accessed 8.21.19).

Colangelo, F., Forcina, A., Farina, I., Petrillo, A., 2018. Life Cycle Assessment (LCA) of Different Kinds of Concrete Containing Waste for Sustainable Construction. Buildings 8, 70. https://doi.org/10.3390/buildings8050070

Dahmen, J., Kim, J., Ouellet-Plamondon, C.M., 2018. Life cycle assessment of emergent masonry blocks. J. Clean. Prod. 171, 1622–1637. https://doi.org/10.1016/j.jclepro.2017.10.044

de Moraes Pinheiro, S.M., Font, A., Soriano, L., Tashima, M.M., Monzó, J., Borrachero, M.V., Payá, J., 2018. Olive-stone biomass ash (OBA): An alternative alkaline source for the blast furnace slag activation. Constr. Build. Mater. https://doi.org/10.1016/j.conbuildmat.2018.05.157

Dolton, B., Hannah, C., 2006. Cellular Concrete : Engineering and Technological Advancement for Construction in Cold Climates 1–11.

Ecoinvent Association, 2019. Ecoinvent database version 3 [WWW Document]. URL https://www.ecoinvent.org/database/database.html (accessed 8.14.19).

Esmaily, H., Nuranian, H., 2012. Non-autoclaved high strength cellular concrete from alkali activated slag. Constr. Build. Mater. 26, 200–206. https://doi.org/10.1016/j.conbuildmat.2011.06.010

Font, A., Borrachero, M.V., Soriano, L., Monzó, J., Mellado, A., Payá, J., 2018. New eco-cellular concretes: Sustainable and energy-efficient materials. Green Chem. https://doi.org/10.1039/c8gc02066c

Font, Alba, Borrachero, M.V., Soriano, L., Monzó, J., Payá, J., 2017. Geopolymer eco-cellular concrete (GECC) based on fluid catalytic cracking catalyst residue (FCC) with addition of recycled aluminium foil powder. J. Clean. Prod. 168, 1120–1131. https://doi.org/10.1016/j.jclepro.2017.09.110

Font, A., Soriano, L., de Moraes Pinheiro, S.M., Tashima, M.M., Monzó, J., Borrachero, M.V., Payá, J., 2020. Design and properties of 100% waste-based ternary alkali-activated mortars: Blast furnace slag, olive-stone biomass ash and rice husk ash. J. Clean. Prod. 243. https://doi.org/10.1016/j.jclepro.2019.118568

Font, A., Soriano, L., Moraes, J.C.B., Tashima, M.M., Monzó, J., Borrachero, M.V., Payá, J., 2017. A 100% waste-based alkali-activated material by using olive-stone biomass ash (OBA) and blast furnace slag (BFS). Mater. Lett. 203. https://doi.org/10.1016/j.matlet.2017.05.129

Funfación Conama - Grupo de trabajo GT-6, 2018. Economía circular en el sector de la construcción. Congr. Nac. del Medio Ambient. 2018.

Hajimohammadi, A., Ngo, T., Mendis, P., Kashani, A., van Deventer, J.S.J., 2017. Alkali activated slag foams: The effect of the alkali reaction on foam characteristics. J. Clean. Prod. 147, 330–339. https://doi.org/10.1016/j.jclepro.2017.01.134

Hassan, H.S., Abdel-Gawwad, H.A., García, S.R.V., Israde-Alcántara, I., 2018. Fabrication and characterization of thermally-insulating coconut ash-based geopolymer foam. Waste Manag. 80, 235–240. https://doi.org/10.1016/j.wasman.2018.09.022

He, Juan, Gao, Q., Song, X., Bu, X., He, Junhong, 2019. Effect of foaming agent on physical and mechanical properties of alkali-activated slag foamed concrete. Constr. Build. Mater. 226, 280–287. https://doi.org/10.1016/j.conbuildmat.2019.07.302

Hogeling, J., Derjanecz, A., 2018. The 2nd recast of the Energy Performance of Buildings Directive (EPBD). Sustain. Dev. 1–30.

IDAE, 2019. Base de datos - Consumo y Emisiones de CO2 en Vehículos Nuevos [WWW Document]. Inst. para la Divers. y Ahorr. la Energía - Gob. España. URL https://www.idae.es/bases-de-datosherramientas (accessed 8.10.19).

IEEE STANDARDS ASSOCIATION, 1981. IEEE 442-1981 - IEEE Guide for Soil Thermal Resistivity Measurements [WWW Document].

IPCC, 2006. Introducción a las Directrices de 2006 1–13.

Kamseu, E., Ngouloure, Z.N.M., Ali, B.N., Zekeng, S., Melo, U.C., Rossignol, S., Leonelli, C., 2015. Cumulative pore volume, pore size distribution and phases percolation in porous inorganic polymer composites: Relation microstructure and effective thermal conductivity. Energy Build. 88, 45–56. https://doi.org/10.1016/j.enbuild.2014.11.066

Keawpapasson, P., Tippayasam, C., Ruangjan, S., Thavorniti, P., Panyathanmaporn, T., Fontaine, A., Leonelli, C., Chayasuwan, D., 2014. Metakaolin-Based Porous Geopolymer with Aluminium Powder. Key Eng. Mater. 608, 132–138. https://doi.org/10.4028/www.scientific.net/KEM.608.132

Luukkonen, T., Abdollahnejad, Z., Yliniemi, J., Kinnunen, P., Illikainen, M., 2018a. One-part alkali-activated materials: A review. Cem. Concr. Res. https://doi.org/10.1016/j.cemconres.2017.10.001

Luukkonen, T., Abdollahnejad, Z., Yliniemi, J., Kinnunen, P., Illikainen, M., 2018b. Comparison of alkali and silica sources in one-part alkali-activated blast furnace slag mortar. J. Clean. Prod. 187, 171–179. https://doi.org/10.1016/j.jclepro.2018.03.202

Ma, C., Zhao, B., Guo, S., Long, G., Xie, Y., 2019. Properties and characterization of green one-part geopolymer activated by composite activators. J. Clean. Prod. 220, 188–199. https://doi.org/10.1016/j.jclepro.2019.02.159

Mak, S., Seo, S., Ambrose, M., Gesthuizen, L., 2008. Sustainable Housing using lightweight cellular concrete. Proc. World Conf. SB08 314–321.

Mellado, A., Catalán, C., Bouzón, N., Borrachero, M. V., Monzó, J.M., Payá, J., 2014. Carbon footprint of geopolymeric mortar: study of the contribution of the alkaline activating solution and assessment of an alternative route. RSC Adv. 4, 23846–23852. https://doi.org/10.1039/C4RA03375B

Ministerio de Fomento - Gobierno de España, 2018. CTE-HE. Código Técnico de la Edificación. Basic document HE (Energy saving). June 68.

Moraes, J.C.B., Font, A., Soriano, L., Akasaki, J.L., Tashima, M.M., Monzó, J., Borrachero, M.V., Payá, J., 2018. New use of sugar cane straw ash in alkali-activated materials: A silica source for the preparation of the alkaline activator. Constr. Build. Mater. 171. https://doi.org/10.1016/j.conbuildmat.2018.03.230

Moreno-Ruiz E., Valsasina L., FitzGerald D., Brunner F., Symeonidis A., Bourgault G., G., W., 2019. Documentation of changes implemented in ecoinvent database v3.6.

Novais, R.M., Buruberri, L.H., Seabra, M.P., Bajare, D., Labrincha, J.A., 2016. Novel porous fly ash-containing geopolymers for pH buffering applications. J. Clean. Prod. 124, 395–404. https://doi.org/10.1016/j.jclepro.2016.02.114

Novais, R.M., Senff, L., Carvalheiras, J., Seabra, M.P., Pullar, R.C., Labrincha, J.A., 2019. Sustainable and efficient cork - inorganic polymer composites_ An innovative and eco-friendly approach to produce ultra-lightweight and low thermal conductivity materials. Cem. Concr. Compos. 97, 107–117. https://doi.org/10.1016/j.cemconcomp.2018.12.024

Peys, A., Rahier, H., Pontikes, Y., 2016. Potassium-rich biomass ashes as activators in metakaolin-based inorganic polymers. Appl. Clay Sci. 119, 401–409. https://doi.org/10.1016/j.clay.2015.11.003

Puertas, F., Torres-Carrasco, M., 2014. Use of glass waste as an activator in the preparation of alkali-activated slag. Mechanical strength and paste characterisation. Cem. Concr. Res. 57, 95–104. https://doi.org/10.1016/j.cemconres.2013.12.005

Pytlik, E.C., Saxena, J., 1992. Autoclaved Cellular Concrete: the Building Material for the 21St Century. Proc. 3rd RILEM Int. Symp. Autoclaved Aerated Concr. 18.

Robayo-salazar, R.A., Robayo-salazar, R., Mejía-arcila, J., Mejía, R., Gutiérrez, D., Martínez, E., 2018. Life cycle assessment (LCA) of an alkali-activated binary concrete based on natural volcanic pozzolan : A comparative analysis to OPC concrete Life cycle assessment (LCA) of an alkali-activated binary concrete based on natural volcanic pozzolan : A co. Constr. Build. Mater. 176, 103–111. https://doi.org/10.1016/j.conbuildmat.2018.05.017

Schroeder, P., Anggraeni, K., Weber, U., 2018. The Relevance of Circular Economy Practices to the Sustainable Development Goals: Circular Economy and SDGs. J. Ind. Ecol. https://doi.org/10.1111/jiec.12732

Stoleriu, S., Vlasceanu, I.N., Dima, C., Badanoiu, A.I., Voicu, G., 2019. Alkali activated materials based on glass waste and slag for thermal and acoustic insulation. Mater. Construcción 69, 194. https://doi.org/10.3989/mc.2019.08518

Sturm, P., Gluth, G.J.G., Brouwers, H.J.H., Kühne, H.C., 2016. Synthesizing one-part geopolymers from rice husk ash. Constr. Build. Mater. 124, 961–966. https://doi.org/10.1016/j.conbuildmat.2016.08.017

Van Den Heede, P., De Belie, N., 2012. Environmental impact and life cycle assessment (LCA) of traditional and “green” concretes: Literature review and theoretical calculations. Cem. Concr. Compos. 34, 431–442. https://doi.org/10.1016/j.cemconcomp.2012.01.004

Xuan, D., Tang, P., Poon, C.S., 2019. MSWIBA-based cellular alkali-activated concrete incorporating waste glass powder. Cem. Concr. Compos. 95, 128–136. https://doi.org/10.1016/j.cemconcomp.2018.10.018

Yang, K.H., Lee, K.H., Song, J.K., Gong, M.H., 2014. Properties and sustainability of alkali-activated slag foamed concrete. J. Clean. Prod. 68, 226–233. https://doi.org/10.1016/j.jclepro.2013.12.068

Zabalza Bribián, I., Valero Capilla, A., Aranda Usón, A., 2011. Life cycle assessment of building materials: Comparative analysis of energy and environmental impacts and evaluation of the eco-efficiency improvement potential. Build. Environ. 46, 1133–1140. https://doi.org/10.1016/j.buildenv.2010.12.002

Ziegler, D., Formia, A., Tulliani, J.M., Palmero, P., 2016. Environmentally-friendly dense and porous geopolymers using fly ash and rice husk ash as raw materials. Materials (Basel). 9. https://doi.org/10.3390/ma9060466